

# Fast Histogram Equalization for Medical Image Enhancement

Qian Wang, Liya Chen, Dinggang Shen\*

**Abstract**—To overcome the problem that the histogram equalization can fail for discrete images, a local-mean based strict pixel ordering method has been proposed recently, although it is unpractical for 3D medical image enhancement due to its complex computation. In this paper, a novel histogram mapping method is proposed. It uses a fast local feature generation technique to establish a combined histogram that represents voxels' local means as well as grey levels. Different sections of the combined histogram, separated by individual peaks, are independently mapped into the target histogram scale under the constraint that the final overall histogram should be as uniform as possible. By using this method, the speed of histogram equalization is dramatically improved, and the satisfactory enhancement results are also achieved.

## I. INTRODUCTION

HISTOGRAM equalization is a widely used technique for image enhancement. When an image is equalized, its grey levels should spread till the margins of the entire scale. Also, the pixel number at each grey level should be made as close as possible. Thereby, the new image after equalization would possibly render better contrast effect for human vision, and details in some dark or bright regions could also show up. For continuous images, histogram equalization is relatively simple to complete, and owns exact solution. However, for discrete images, things become different. Usually, several minor grey levels would merge into only one grey level if the discrete images were equalized in the same way as the continuous images. More importantly, the details included in the minor grey levels will be lost after image equalization, although equalization itself is supposed to make details clearer after enhancement.

Many attempts have already been made for digital image histogram equalization. A prevalent method is to order all pixels contained in an image, and then to equally separate those ordered pixels into groups of the same number of pixels. Finally, all pixels in the same group will be assigned with a same new grey level value which gradually changes from the beginning of the target grey level scale to the end, and the new image with uniform histogram can be generated. In [1], several local means generated from different sizes of neighborhoods were employed to strictly differentiate and

order pixels with the same intensity. For example, three different local means can be generated for each pixel using the masks defined in Fig. 1. Suppose  $P = \{p_0, p_1, \dots, p_{n-1}\}$  is the set of pixels contained in an image. To order any two pixels  $p_i$  and  $p_j$ , we need first refer to their grey levels. If their grey levels are different, we can easily obtain  $p_i < p_j$  or  $p_j < p_i$ . But if the grey levels are the same, we have to check their first local means defined by the mask in the left panel of Fig. 1. If they are still not distinguishable, we have to check their next local means, or even further ones, until they can be separated. In this way, we could finally order all pixels of the image. That means, the set  $P$  can be finally transformed into  $P' = \{p'_0, p'_1, \dots, p'_{n-1} | p'_0 < p'_1 < \dots < p'_{n-1}\}$ . This new set can be easily divided into groups of the same number of pixels, while pixels in the same group can be assigned with a same new grey level.

This local-mean based strict ordering method is applicable for equalization of 2D images. However, it is clinically not feasible when applied to the 3D medical images, since the strict ordering [2] of millions of voxels requires extremely long processing time. To solve this problem, an efficient histogram equalization method is developed, as detailed next.

$$\frac{1}{5} \begin{bmatrix} 0 & 1 & 0 \\ 1 & 1 & 1 \\ 0 & 1 & 0 \end{bmatrix} \quad \frac{1}{9} \begin{bmatrix} 1 & 1 & 1 \\ 1 & 1 & 1 \\ 1 & 1 & 1 \end{bmatrix} \quad \frac{1}{13} \begin{bmatrix} 0 & 0 & 1 & 0 & 0 \\ 0 & 1 & 1 & 1 & 0 \\ 1 & 1 & 1 & 1 & 1 \\ 0 & 1 & 1 & 1 & 0 \\ 0 & 0 & 1 & 0 & 0 \end{bmatrix}$$

Fig. 1. Masks employed in Coltuc's method [1].

## II. METHODS

In our method, grey level transformation (or mapping) is *histogram-based* rather than *voxel-based*. Unlike [1] [3], our method does not require the strict ordering of voxels at all. In fact, it just simply maps a combined histogram, which is represented by a histogram tree, to the new target grey level scale, by simultaneously keeping the final overall histogram as uniform as possible. Compared to the regional adaptive histogram equalization methods such as in [4], our method performs histogram mapping only once by direct incorporation of global and local features into a histogram tree, while those regional adaptive methods generally need to perform regional histogram transformations voxel by voxel, thus the global image structure might not be well respected.

Similar to Coltuc's method in [1], we need to firstly generate local features for each voxel in the original image under consideration for equalization. Although in [1] [3],

Qian Wang is with the Department of Electronic Engineering, Shanghai Jiao Tong University, Shanghai, 200240, China (phone: 86-21-34205281; e-mail: wang.qian@sjtu.edu.cn).

Liya Chen is with the Department of Electronic Engineering, Shanghai Jiao Tong University, Shanghai, 200240, China (phone: 86-21-34204640; e-mail: liyachen@sjtu.edu.cn).

Dinggang Shen is with the Department of Radiology and BRIC, The University of North Carolina at Chapel Hill, NC 27510 (e-mail: dgshen@med.unc.edu). \*Corresponding author.

several ways have been proposed to effectively extract local features, we instead employ recursive Gaussian filters [5] to fulfill this goal. Compared to the classical method of smoothing an image by convolution with a Gaussian kernel, this novel filter implements an approximation of convolution with the Gaussian kernel and its derivatives by using IIR filters. Thus, the drawback of heavy computation per voxel with the conventional method could be under control, since the computation in our implementation is not related with the size  $\sigma$  of the Gaussian kernel used. In Fig. 2(a), a typical slice of an abdomen CT volume is shown. The results after being smoothed by the recursive Gaussian filters are shown in Fig. 2(b) and (c). More blur image is produced after using a larger neighborhood size (Fig. 2(c)). By gradually changing the sets of parameters, we can easily get a series of smoothed images with larger and larger neighborhood sizes. For any given voxel  $p_i$ , its local feature could be described by vector  $D_{p_i} = (G_{p_i}, L_{1,p_i}, L_{2,p_i}, \dots)$ , where  $G_{p_i}$  denotes the original grey level and  $L_{t,p_i}$  denotes the corresponding value on the  $t$ -th smoothed image.

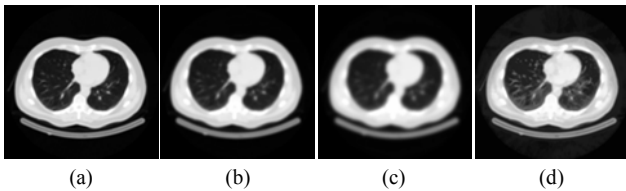


Fig. 2. (a): A typical slice of an abdomen CT volume; (b) and (c): Results after smoothing by recursive Gaussian filters with different sets of parameters; (d): Equalization result.

By using local feature vectors, we can create a tree of histograms for each image, as described next. *First*, a parent (regular) histogram based on the original grey levels can be built. *Then*, for each bin in this histogram, we can generate a child histogram to represent the distribution of the first local feature/mean ( $L_1$ ) of those voxels contained in the same parent bin as shown in Fig. 3. In our test, it proves that a 3-level histogram tree is sufficient for well separation of voxels in most images. That means, for a given voxel  $p_i$ , we need to take advantage of its local feature vector  $(G_{p_i}, L_{1,p_i}, L_{2,p_i})$ . Since local features/means generally do not vibrate far away from the original grey level ( $G$ ), we can truncate those child histogram's bins with values too far away from the original grey level ( $G$ ) of the respective parent bins, such as  $|L_1 - G| > r$  or  $|L_2 - G| > r$  ( $r$  denotes the manually set maximal allowable offset between original grey level and local feature/mean), for the purpose of smaller memory allocation and better speed performance. In Fig. 3 for example, suppose the grey level  $G = g$ , the set of its reserved child bins will only contain the elements whose local means are between  $g - r$  and  $g + r$ , and those bins outside the dotted fillet rectangle will be truncated from the histogram tree. The contributions to the histogram tree from the voxels belonging to the truncated bins will be simply counted on the

marginal bins such as  $(G = g, L_1 = g \pm r, L_2 = g \pm r)$ . After that, we could get two histograms, i.e., the *regular histogram* composed of grey level bins, and the *combined histogram* which is composed of all the reserved leaf bins of the last level in Fig. 3.

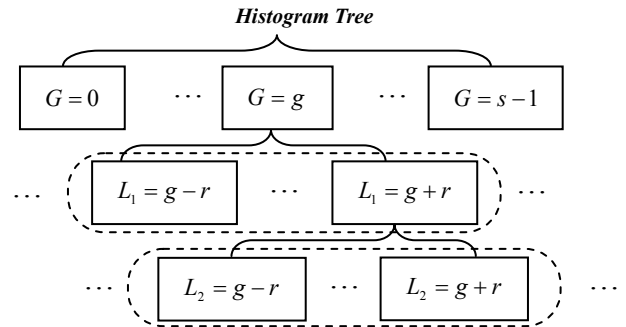


Fig. 3. A 3-level histogram tree. In the lower 2 levels, only bins contained in the dotted fillet rectangle are reserved, while others are truncated since they denote local features/means owned by few voxels.

There usually exist some peaks and valleys in both the regular and the combined histograms, and different peaks generally imply different anatomical structures in medical images [6]. Suppose a simple regular histogram as in Fig. 4(a) where the 3 bins from left to right contain respectively 33.3%, 16.7%, 50% of total voxels, and the corresponding combined histogram is shown in Fig. 4(b) where 3 peaks are contained. If directly applying traditional equalization to the combined histogram, we would observe inter-peak interference (IPI) indicated by the dashed arrow in Fig. 4(c): some bins of Peak 1 originally would be exiled and combined to Peak 2, in order that new Peak 1 and 2 after equalization own the same number of voxels and spread the same scale of target grey levels. However, the result in Fig. 4(c) diminishes the marginal contrast between the two structures implied by Bins 1 and 2: after equalization a part of voxels belonging to Bin 1 would be assigned with grey levels so close to Bin 2's voxels that they might not even be distinguished. If the two bins just imply spatially neighboring structures, IPI could greatly destroy the edge information after equalization.

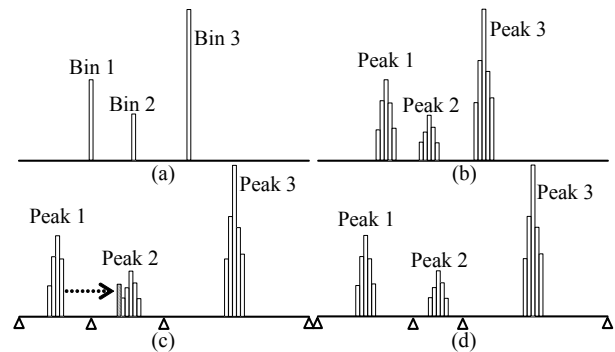


Fig. 4. (a): A simple regular histogram; (b): The corresponding combined histogram; (c): Equalization without peak segmentation: IPI occurs as indicated by the dashed arrow; (d): Equalization with peak segmentation.

In order to prevent IPI, we will segment the combined

histogram into several sections, each containing just one peak. The following equalization will be restricted to each section only as in Fig. 4(d) so that no IPI will occur. To fulfill this, the regular histogram is first processed to locate peaks and generate sections [7]. For example, Fig. 5 shows the regular histogram of the abdomen CT image shown in Fig. 2, and the dotted line represents the signs of the *peak detection signals* (PDS). By identifying the zero-crossings of PDS, the peaks of the regular histogram can be located individually. In particular, the negative zero-crossing (crossing from positive to negative), or its cluster, indicates the start position or the end position of a peak, e.g., those pointed by arrows 1 and 3 in Fig. 5, while the positive zero-crossing (crossing from negative to positive), or its cluster, indicates the exact peak location, e.g., those pointed by arrows 2 [7]. For the  $k$ -th peak section  $\{S_k, E_k\}$  that starts at  $S_k$  and ends at  $E_k$  on the regular histogram, its mirrored section  $\{S'_k, E'_k\}$  on the combined histogram could be easily located based on the criterion that the grey levels at the ends of  $\{S'_k, E'_k\}$  should equal to the grey levels of  $S_k$  and  $E_k$ , respectively.

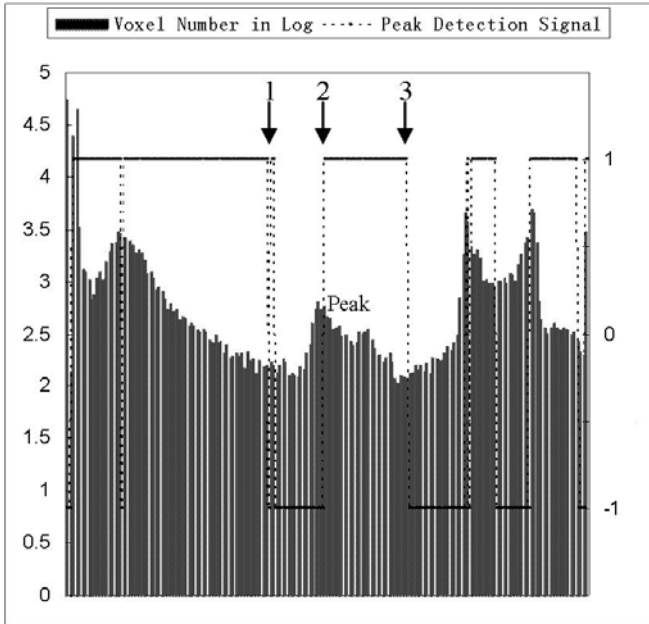


Fig. 5. The regular histogram of the abdomen CT volume shown in Fig. 2(a) and its PDS signs (dotted line). Arrow 1 points to a cluster of negative zero-crossings which indicates the start position of a specific peak, while arrow 3 points a negative zero-crossing indicating the end position of the peak. And arrow 2 points to a positive crossing which indicates the exact peak location.

Finally, a recursive mapping creator is employed to map each section of the combined histogram into its corresponding target histogram section. In particular, for a section  $\{S'_k, E'_k\}$  in the combined histogram, its mapped section in the target histogram can be denoted as  $\{S''_k, E''_k\}$  with the span  $d = E''_k - S''_k$  proportional to the number of voxels contained in the source section  $\{S'_k, E'_k\}$ . Usually, if not always, the number of bins contained in the source section is much larger than that in the target section, since each grey

level in the original image corresponds to tens of bins in the combined histogram which integrates the information of both grey levels and local features/means. To map the source section  $\{S'_k, E'_k\}$  into the target section  $\{S''_k, E''_k\}$  for instance, both of these two sections will be first divided into two parts. Note, the two parts of  $\{S'_k, E'_k\}$  will own the equal number of *voxels*, while the two parts of  $\{S''_k, E''_k\}$  will own the equal number of *grey levels*. The first part of  $\{S'_k, E'_k\}$  and the first part of  $\{S''_k, E''_k\}$  will become the new source-target pair, and so is to their pair of the second parts. This method will be recursively performed until each grey level in  $\{S''_k, E''_k\}$  can be connected to its source, i.e., a part of the original source section  $\{S'_k, E'_k\}$ . After completing this process of histogram mapping, each voxel in the original image can find a new grey level in the target histogram; thus, the original image can be equalized. In Fig. 2(d), we can see the enhancement result of the slice in Fig. 2(a), after using our equalization method.

In all, the proposed fast histogram equalization method could be summarized as following:

- 1) Local features/means of the image to be equalized are generated using recursive Gaussian filters. Both the *regular* and the *combined* histograms could be established based on grey levels in the image and its generated local features/means.
- 2) The combined histogram is decomposed into several sections each of which contains only one peak. For a specific section, it would be connected with the corresponding grey level scale on the target histogram.
- 3) Inside a single pair of the section on the combined histogram and the target scale, recursive mapping would be performed. Then the equalized image could be generated.

### III. RESULTS

We have performed several tests to demonstrate the performance of the proposed image enhancement method. As demonstrated next, compared to the strict ordering methods [1], the proposed method is faster to complete, along with desired performance.

#### A. Performance of Image Enhancement



Fig. 6. (a) The original Lena image; (b) The equalization result using our method; (c) The equalization result using Coltuc's strict ordering method [1].

Lena image is used here to demonstrate the performance of image enhancement, as shown in Fig. 6. Fig. 6(a) is the

original Lena image, while Fig. 6(b) is the result after equalization using our method. Fig. 6(c) is the result after equalization using Coltuc’s strict ordering method [1]. Visually, these two image enhancement results are similar, which indicates that the performance of our method is not worsened with the improvement of speed as reported next.

### B. Robustness to Noise

Two simulated brain MRI images [8] (as shown in Fig. 7) are used to demonstrate the robustness of the proposed method to noise. Fig. 7(a) is the original image, and the corresponding image with addition of 40% Gaussian noise is shown in Fig. 7(c). The enhancement results of these two images are shown in Fig. 7(b) and (d), respectively, which confirms the robustness of the proposed method. For example, even with strong noise, some details hidden in dark or bright regions can still be enhanced in the noisy image.

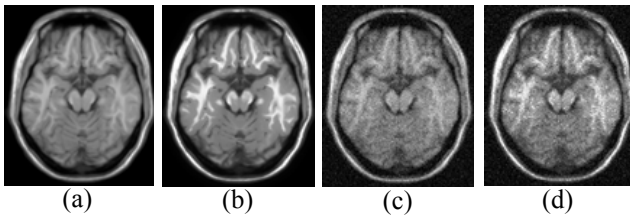


Fig. 7. Robustness of the proposed method to noise. (a): A slice of a simulated brain MRI volume; (b): Enhancement result of (a); (c): A noisy image generated from (a); (d): Equalization result of (c).

### C. Speed

In the beginning of this paper, we have mentioned that, if a strict ordering method is used for the enhancement of 3-D images, it takes too long time. In Table 1, we provide a series of quantitative values to compare the speeds of this method with our proposed method in enhancement of 2-D and 3-D images. As demonstrated, the speed of our proposed method can be dramatically improved.

TABLE I  
SPEED COMPARISON BETWEEN TWO METHODS

Sample	Size (voxels)	Time Cost (sec)	
		Our Method	Coltuc’s Method
Lena	256×256	0.96	2.45
Lung X-ray	256×256	0.91	2.33
Abdomen CT	512×512×25	12.54	182.57
Brain MRI	181×217×181	17.69	235.24

Four types of images have been used to compare the speeds between our method and Coltuc’s method [1]. For 2-D images, such as Lena and Lung X-ray images, our method can improve speed by about 2.5 times. For 3-D images that contain a great number of voxels, our method can improve speed dramatically. The task to equalize the abdomen CT or brain MRI volume is rather challenging for Coltuc’s method [1], and the estimated time cost to process a single volume is at least longer than 3 minutes. On the other hand, by using our method, it took extremely less time (<20s) to equalize a 3-D volume with the size of 512×512×25 or 181×217×181 voxels.

The reason is that Coltuc’s method has to order the millions of voxels based on their grey levels as well as local means, whereas, in our method, it only needs to generate and process a histogram tree. Suppose that there are  $l=3$  levels in the histogram tree, and the allowable maximal offset is  $r=5$ . Then, the combined histogram only has  $(2r+1)^{l-1} \cdot s = 121s$  independent bins, where  $s$  is the total number of grey levels in the original image. The bin number (121s) is generally much smaller than the number of voxels in the 3-D images, thus the computation in our method can be effectively decreased.

## IV. CONCLUSION

We have presented a fast image equalization method by constructing a histogram tree with direct incorporation of both original grey levels and local means of multiple scales. The experimental results show that the proposed method owns the enhancement performance close to that achieved by a strict ordering method [1], while the enhancement speed is dramatically improved. In the future, we will apply this method to more types of medical images to evaluate its performance. Also, we will further improve its speed, for possible real-time medical applications.

In the future, we will investigate an accurate and external criterion to help judge whether a specific image or its internal region needs to be equalized and enhanced. Moreover, certain machine learning methods might be employed to make the process of parameter tuning automatic.

## REFERENCES

- [1] D Coltuc, P Bolon, JM Chassery, “Exact Histogram Specification”, *IEEE Trans. on Image Processing*, vol. 15, no. 5, pp. 1143-1152, May 2006.
- [2] D Coltuc, P Bolon, “Strict Ordering on Discrete Images and Applications”, *Proc. ICIP 99*, vol. 3, pp. 150-153, 1999.
- [3] Y Wan, D Shi, “Joint Exact Histogram Specification and Image Enhancement Through the Wavelet Transform”, *IEEE Trans. on Image Processing*, vol. 16, no. 9, pp. 2245-2250, September 2007.
- [4] JA Stark, “Adaptive Image Contrast Enhancement Using Generalizations of Histogram Equalization”, *IEEE Trans. on Image Processing*, vol. 9, no. 5, pp. 889-896, May 2000.
- [5] R Deriche, “Fast Algorithms for Low-Level Vision”, *IEEE Trans. on Pattern Analysis and Machine Intelligence*, vol. 12, no. 1, pp. 78-87, January 1990.
- [6] GW Davis, ST Wallenslager, “Improvement of Chest Region CT Images through Automated Gray-Level Remapping”, *IEEE Trans. on Medical Imaging*, vol. 5, no. 1, pp. 30-34, June 1986.
- [7] MI Sezan, AM Teklap, R Schaetzing, “Automatic Anatomically Selective Image Enhancement in Digital Chest Radiography”, *IEEE Trans. on Medical Imaging*, vol. 8, no. 2, pp. 154-162, June 1989.
- [8] CA Cocosco, V Kollokian, RK-S Kwan, GB Pike, AC Evans, “BrainWeb: Online Interface to a 3D MRI Simulated Brain Database”, *NeuroImage*, vol. 5, no. 4, part 2/4, S425, 1997.